GROWTH CONDITIONS AND GENESIS OF SPHERICAL AND PLATY KAOLINITE

SHINJI TOMURA, YASUO SHIBASAKI, HIROYUKI MIZUTA

Government Industrial Research Institute, Nagoya
1 Hirate-cho, Kita-ku, Nagoya 462, Japan

MASAO KITAMURA

Department of Geology and Mineralogy, Faculty of Science
Kyoto University, Sakyo-ku, Kyoto 606, Japan

Abstract—Spherical and platy kaolinite crystals were prepared under several hydrothermal conditions. Spherical kaolinite was produced mainly at high solid/water ratio (1/4) and at low temperatures (150°–200°C). Platy kaolinite predominated in products from experiments with intermediate solid/water ratios (1/256–1/16) and at high temperatures. Boehmite predominated at low solid/water ratios (1/4096) at all experimental temperatures (180°–220°C). The results indicate that the growth of the spherical kaolinite was favored at high degrees of supersaturation, whereas the growth of the platy kaolinite was favored at relatively low degrees of supersaturation.

要旨 — 球状及び板状カオリナイトを種々の水熱条件下で合成した。球状カオリナイトは高濃度（原料／水＝1／4）低温度（150°～200°C ）で良く生成した。板状カオリナイトは中間の濃度（原料／水＝1／256～1／16 ）高温度（220°C ）で良く生成した。その他、ベーマイトが低濃度（1／4096）で広い温度範囲（180～220°C ）で生成した。これらの結果から、球状カオリナイトは高い過飽和状態で良く生成し、板状カオリナイトは相対的に低い過飽和度状態で生成すると考えられた。

Key Words—Crystal growth, Kaolinite, Morphology, Plates, Spherules, Synthesis.

INTRODUCTION

Morphology has been used to distinguish different members of the kaolin group of minerals. Platy kaolinite, tubular halloysite, and spherical halloysite have been recognized in diverse geologic environments, and their formation mechanisms have been studied by many investigators (e.g., Dixon and McKee, 1974; Sudo and Yotsumoto, 1977; Kirkman, 1981). Recently, Tomura *et al.* (1983) produced still another morphological variety in the form of spherical kaolinite. Inasmuch as morphology is of fundamental importance to the mineralogy of the kaolin-group minerals, it is worthwhile to examine the precipitation processes that produce such morphological variations.

The precipitation of kaolinite from crystalline or noncrystalline aluminosilicates in aqueous solution or under hydrothermal conditions has been discussed from many points of view, including: (1) dissolution and precipitation kinetics (Helgeson, 1971; Tsuzuki and Mizutani, 1971; Tsuzuki *et al.,* 1974); (2) equilibrium relations on activity diagrams (Helgeson, 1968; Helgeson *et al.,* 1969; Kittrick, 1970; Keller *et al.,* 1971; Huang and Keller, 1973; Eberl and Hower, 1975; Tsuzuki, 1976; Busenberg, 1978; La Iglesia and Van Oos-

terwyck-Gastuche, 1978; Tsuzuki and Suzuki, 1980; Tsuzuki and Kawabe, 1983); (3) structure and composition of starting materials (Poncelet and Brindley, 1967; De Kimpe and Fripiat, 1968; Trichet, 1969; Oberlin and Couty, 1970; Urabe *et al.,* 1970; Rodrique *et al.,* 1972; De Vijnck, 1973); and (4) coordination number or polymerization state of hydrated species (De Kimpe *et al.,* 1961; De Kimpe and Gastuche, 1964; Polzer *et al.,* 1967; Linares and Huertas, 1971; La Iglesia and Martin Vivaldi, 1973; Hem and Lind, 1974; La Iglesia and Galan, 1975; Lind and Hem, 1975; La Iglesia *et al.,* 1976; De Kimpe *et al.,* 1981). A detailed review of this subject was given by Van Oosterwyck-Gastuche and La Iglesia (1978).

In the present experiment, the growth of spherical kaolinite and the transformation of spherical kaolinite into platy kaolinite was studied as a function of run duration and the solid/water ratio of the starting material.

EXPERIMENTAL

Hydrothermal synthesis

Starting materials were prepared by the same method as described previously (Tomura *et al.,* 1983), that

Table 1. Summary of the results of experiment 1, the effect of the starting solid/water ratio.[1]

| Run temp. (°C) | Start. solid/ water ratio | Products[2] | Surface area (m²/g) | Estimated amount of particles[3] | | | | SK |
				NC (%)	B (%)	SK (%)	PK (%)	(SK + PK) (%)
180	1/4096	NC + B	266	43	57	0	0	—
	1/1024	NC + K	278	92	0	0	8	0
	1/256	NC + K	196	97	0	3	0	100
	1/64	NC	167	100	0	0	0	—
	1/16	NC	158	100	0	0	0	—
	1/4	NC	148	100	0	0	0	—
200	1/4096	NC + B	248	10	90	0	0	—
	1/1024	NC + K	267	74	0	3	23	12
	1/256	NC + K	104	19	0	28	53	35
	1/64	NC + K	109	49	0	18	33	35
	1/16	NC + K	105	65	0	14	21	40
	1/4	NC + K	112	70	0	25	5	83
220	1/4096	NC + B	146	6	94	0	0	—
	1/1024	NC + K + B	188	54	7	0	38	0
	1/256	NC + K	41	31	0	7	62	10
	1/64	NC + K	69	62	0	2	36	5
	1/16	NC + K	94	67	0	2	31	6
	1/4	NC + K	100	68	0	4	28	13

[1] Run time and Al/Si ratio of starting materials were fixed to 96 hr and 1/1, respectively.
[2] Determined by X-ray powder diffraction analysis. NC = noncrystalline aluminosilicate; K = kaolinite; B = boehmite.
[3] Estimated from the data of X-ray powder diffraction analysis, electron microscopy, and differential thermogravimetry (see text). SK = spherical kaolinite; PK = platy kaolinite.

is, a mixed sol of colloidal silica and alumina was prepared in an atomic ratio of Al/Si = 1. The sol was spray-dryed and calcined at 600°C.

In experiment 1, 0.4883, 1.9531, 7.8125, 31.25, 125, and 500 g of starting material and 2000 ml of distilled water were placed in a 3-liter, Teflon bottle. Weight ratios of solid/water were thus 1/4096, 1/1024, 1/256, 1/64, 1/16, and 1/4, respectively. The bottle was sealed in a 10-liter, stainless steel pressure vessel. Prior to the sealing of the pressure vessel, 1000 ml of distilled water was placed around the Teflon bottle to avoid the evaporation of water in the bottle. The pressure vessel was maintained at temperatures of 180°, 200°, and 220°C for 96 hr. The pressure was the equilibrium water pressure at the corresponding temperature.

In experiment 2, 4 g of starting material and 16 ml of distilled water were sealed in a 25-ml, stainless steel, Teflon-lined (for runs ≤250°C) or nonlined (for runs ≥280°C) Morey-type pressure vessel. The pressure vessel was maintained at temperatures of 150°, 180°, 200°, 220°, 250°, 280°, and 300°C for periods of 2 to 1488 hr according to the rate of reaction.

Measurements

Products were characterized by X-ray powder diffraction (XRD), differential thermal analysis (DTA), differential thermogravimetry (DTG), and specific surface area measurements, and by conventional transmission (TEM) and analytical electron microscopy

(AEM) according to the procedures previously described by Tomura et al. (1983).

The ratio of (kaolinite + boehmite)/noncrystalline material in the products was estimated from the DTG weight-loss peak at 550°C which was attributed to the decomposition of kaolinite and boehmite. Because of overlapping of kaolinite and boehmite DTG peaks, the kaolinite:boehmite ratio was estimated from the intensities of the 001 reflection of kaolinite and the 020 reflection of boehmite in the XRD pattern.

The ratio of platy kaolinite to spherical kaolinite was estimated from areal ratio of these minerals on electron micrographs and raised to the 3/2 power to convert it to volume or weight ratio. Finally the ratio of platy kaolinite:spherical kaolinite:boehmite:noncrystalline material was calculated by compiling the above values.

The population density of spherical kaolinite was evaluated from the numbers of spherical kaolinite particles in an unit area as observed on electron micrographs, and then, the value raised to the 3/2 power to convert it into population per unit volume.

Because the boehmite that formed in the present experiments was hexagonal platy, the amount of platy kaolinite may have been overestimated when a combination of XRD and TEM methods was used. Boehmite and platy kaolinite, however, were found to coexist without spherical kaolinite, and platy and spherical kaolinite were found to coexist without boehmite; hence the ratio was estimated by combination of DTG +
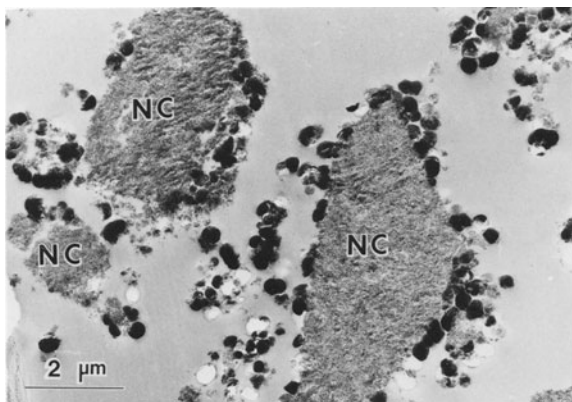
Figure 1. Transmission electron micrograph of ultrathin-sectioned product synthesized at 150°C for 1488 hr. Spherules are formed around the periphery of noncrystalline alumino-silicate (NC).
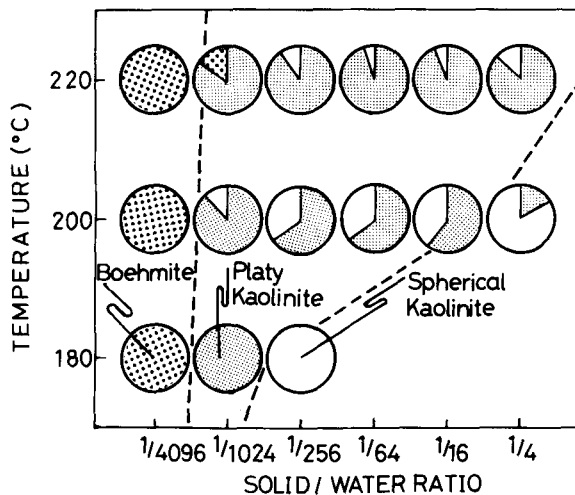

Figure 3. Amount of the precipitated minerals in experiment 1, plotted with temperature as the ordinate and solid/water ratio as the abscissa. Broken lines indicate estimated boundaries between boehmite and platy kaolinite, and between platy kaolinite and spherical kaolinite.

XRD or DTG + TEM, and the possibility of error was minimized.

RESULTS

Results of experiment 1 are summarized in Table 1. Detected species were boehmite, platy kaolinite, spherical kaolinite, and noncrystalline aluminosilicate. In all runs at low solid concentration (solid/water = 1/4096), hexagonal plates of boehmite were precipitated. The ratio of spherical kaolinite to total kaolinite increased with an increase in the solid/water ratio, except for the run with solid/water = 1/256 at 220°C. Spherical kaolinite was not formed within the noncrystalline aluminosilicate particles, but around their periphery (Figure 1).

Table 2 shows the results of experiment 2. Detected species by XRD were kaolinite and noncrystalline ma-

terial. Boehmite was not detected in these products. Observed species under the electron microscope were spherical, platy, and noncrystalline material. The detected species by both methods in the longer runs were consistent if the spherical and platy materials are both considered to be kaolinite. On the other hand, the spherical and platy materials in the shorter runs could not be identified by XRD, likely due to the very small amount of these phases present. Electron diffraction study and analytical electron microscopy of some of the small spherules and platy material formed in the shorter runs indicated that most of these materials were kaolinite. The mean diameter of the spherical kaolinite was 0.05 to 1.01 μm. Increasing the time and temperature led to larger diameters. The population density of spherical kaolinite ranged from 0 to 8.1 particles/μm^3, although this value fluctuated. The morphology of the products of experiment 2 are shown schematically in Figure 2. The change of the kaolinite from

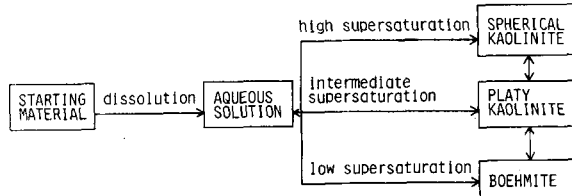Figure 2. Morphological phase diagrams of products obtained in experiment 2.

Figure 4. Dissolution and precipitation process of a starting material into kaolin minerals and boehmite in a hydrothermal solution system. Rates of the precipitation and species of precipitate are influenced by the supersaturation in solution. Supersaturation is influenced by the dissolution rate of the starting material.

Table 2. Summary of results of experiment 2.

Run temp. (°C)	Run time (hr)	Products[1] (XRD)	Products[2] (TEM)	Surface area (m^2/g)	Amount of kaolinite (by DTG)[3] (wt. %)	Mean diameter of spherule (μm)	Population density of spherule (μm^{-3})
150	48	NC	NC	176	0	—	—
	360	NC	NC + S	207	1	0.05	6.2
	720	NC + K	NC + S + P	207	4	0.09	1.8
	984	NC + K	NC + S	206	12	0.19	1.1
	1200	NC + K	NC + S + P	208	20	0.21	2.6
	1488	NC + K	NC + S + P	165	39	0.34	2.8
180	24	NC	NC	150	0	—	—
	48	NC	NC + S	150	0	0.08	0.7
	96	NC	NC + S + P	148	5	0.15	8.1
	192	NC + K	NC + S	138	18	0.23	5.5
	336	NC + K	NC + S + P	97	53	0.33	3.0
	480	NC + K	NC + S + P	59	82	0.42	0.8
	600	NC + K	NC + S + P	49	86	0.42	2.8
	744	NC + K	NC + S + P	38	86	0.43	0.6
200	6	NC	NC	142	0	—	—
	12	NC	NC + S	142	0	0.04	0.1
	16	NC	NC + S	136	0	0.08	0.2
	20	NC	NC + S + P	136	0	0.09	0.6
	24	NC	NC + S + P	145	0	0.11	0.5
	48	NC + K	NC + S + P	140	6	0.18	4.2
	96	NC + K	NC + S + P	124	19	0.30	3.6
	144	NC + K	NC + S + P	104	48	0.33	0.8
	192	NC + K	NC + S + P	70	79	0.37	0.6
	240	NC + K	NC + S + P	86	81	0.41	0.8
	312	NC + K	NC + S + P	41	92	0.40	1.9
	360	NC + K	NC + S + P	37	96	0.43	1.4
	480	NC + K	NC + S + P	38	92	0.38	1.6
	624	K	S + P	40	99	0.37	1.7
220	6	NC	NC	124	0	—	—
	8	NC	NC + S + P	124	0	0.08	0.8
	12	NC	NC + S + P	123	0	0.16	1.6
	16	NC	NC + S + P	124	0	0.20	4.5
	20	NC	NC + S + P	124	0	0.19	7.9
	24	NC + K	NC + S + P	121	3	0.26	1.9
	48	NC + K	NC + S + P	98	20	0.30	0.3
	144	NC + K	NC + S + P	54	93	0.37	0.1
	192	K	S + P	43	98	0.37	<0.1
	336	K	S + P	41	97	0.36	<0.1
	360	K	S + P	43	99	0.37	<0.1
250	3	NC	NC	163	0	—	—
	6	NC	NC	151	0	—	—
	9	NC	NC + S + P	151	0	<0.01	<0.1
	12	NC	NC + S + P	158	0	0.14	0.4
	15	NC + K	NC + S + P	155	2	0.34	0.2
	24	NC + K	NC + S + P	158	11	0.59	0.1
	36	NC + K	NC + S + P	95	70	0.56	0.1
	48	K	S + P	41	93	0.50	0.1
	72	K	S + P	41	94	0.57	0.1
	96	K	S + P	41	96	0.54	0.1
280	10	NC	NC + S + P	154	0	0.19	0.2
	13	NC	NC + S + P	167	0	0.22	0.6
	16	NC	NC + S + P	154	2	0.52	<0.1
	19	NC + K	NC + S + P	154	9	0.46	<0.1
	22	NC + K	NC + S + P	83	63	0.58	<0.1
	24	NC + K	NC + S + P	102	62	0.61	<0.1
	33	K	S + P	40	92	1.01	<0.1
	48	K	S + P	40	99	0.69	<0.1
	57	K	S + P	39	90	0.54	<0.1
	81	K	S + P	40	91	0.59	<0.1
300	2	NC	NC + S + P	153	0	<0.01	<0.1
	7	NC	NC + S + P	150	0	0.28	0.1

Table 2.   Continued.

Run temp. (°C)	Run time (hr)	Products[1] (XRD)	Products[2] (TEM)	Surface area (m²/g)	Amount of kaolinite (by DTG)[3] (wt. %)	Mean diameter of spherule (μm)	Population density of spherule (μm⁻³)
	12	NC + K	NC + S + P	153	18	0.51	0.3
	25	NC + K	S + P	52	90	0.55	<0.1
	27	K	S + P	42	97	0.51	<0.1
	30	K	S + P	42	95	0.69	<0.1
	36	K	S + P	43	93	0.69	<0.1
	40	K	S + P	42	99	0.98	<0.1
	48	K	S + P	41	97	0.40	<0.1
	96	K	S + P	40	96	0.47	<0.1

[1] Determined by X-ray powder diffraction analysis. NC = noncrystalline material; K = kaolinite.
[2] Determined by transmission electron microscopy. S = spherule; P = platy material.
[3] Differential thermal gravimetry.

spherical to platy was common in runs at all temperatures. Long run times at low temperatures were required to change the morphology.

DISCUSSION

Spherical kaolinite formed only around the periphery of particles of starting material (also see Figure 3 in Tomura *et al.,* 1983), indicating that the spherical kaolinite probably formed by a dissolution-precipitation mechanism.

The proportions of minerals in the products in experiment 1 (Figure 3) suggest that boehmite, platy kaolinite, and spherical kaolinite precipitated mainly at low, intermediate, and high solid/water ratios, respectively. This change from boehmite to kaolinite is consistent with the theoretical activity diagrams of Tsuzuki (1976) and Walter and Helgeson (1977) which shows that the Si concentration of solution at which boehmite precipitates is lower than that for kaolinite. The fact that spherical kaolinite precipitated mainly at

the highest solid/water ratios suggests that the precipitation of this mineral occurred in highly supersaturated solution. The change of the morphology of kaolinite from spherical to platy with an increase in the run time indicates that the spherical form is metastable.

The observed relations between supersaturation and the nature of precipitated minerals are summarized in Figure 4. It is widely accepted that the dissolution rate is proportional to the solid/water ratio where the specific surface area of the starting material is constant (Lasaga, 1981). Therefore, the dissolution rate of a starting material with high solid/water ratio is high. Because the precipitation rate of a mineral is low at low temperature, this solution became highly supersaturated and precipitated spherical kaolinite as a
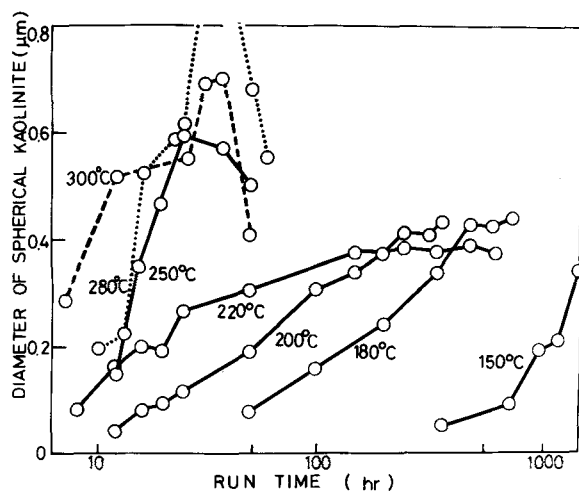

Figure 5.   Mean diameter of spherical kaolinite vs. run time in experiment 2 at different temperatures.
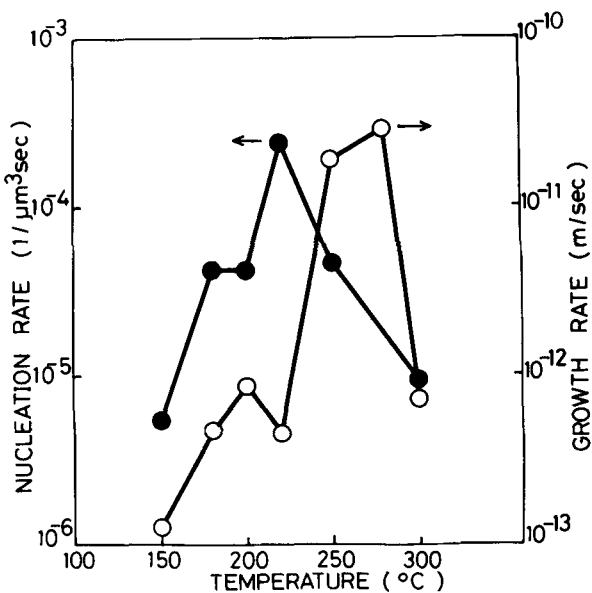

Figure 6.   Linear growth rate (solid circles indicated as right ordinate) and nucleation rate (open circles indicated as left ordinate) of spherical kaolinite vs. run temperature in experiment 2.

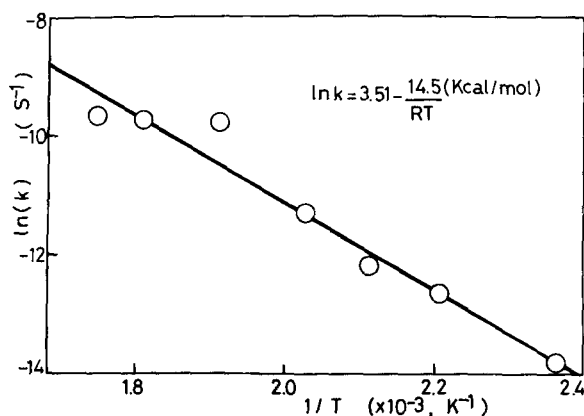$$\ln k = 3.51 - \frac{14.5 (\text{Kcal/mol})}{RT}$$

Figure 7. Arrhenius plot of kaolinite formation from non-crystalline aluminosilicate in experiment 2 on the assumption of autocatalytic reaction kinetics.

metastable form. On the other hand, in the run with a low solid/water ratio at high temperature, the solution was only mildly supersaturated, and boehmite precipitated. Platy kaolinite precipitated at what can be considered to be an intermediate degree of supersaturation. Furthermore, the transformation of early precipitated metastable forms to stable ones must occur with a change in the degree of supersaturation.

To ascertain quantitatively the kinetics of precipitation, the change of the mean diameter of spherical kaolinite was plotted against run time in experiment 2 (Figure 5). Between 150° and 220°C, the mean diameter of the spherical kaolinite increased with run time. In runs at 250°, 280°, and 300°C, the diameter also increased with run time to about 30 hr, but with longer run times it then decreased. This decrease in diameter indicates that the spherical kaolinite was metastable at these temperatures.

From the initial slope of each curve, linear growth rates along the radius of the spherical kaolinite were obtained (Figure 6). Also, from the initial slope of the population density curve, the nucleation rates of spherical kaolinite were obtained and plotted in Figure 6. In runs above 250°C, the growth rate of spherical kaolinite was high, but the nucleation rate was low, which resulted in a small number of large kaolinite spheres. In runs below 220°C, the growth rate was smaller than at higher temperatures, and nucleation rate was at a maximum. In these runs, many small kaolinite spheres were formed.

The apparent kinetic constant (k) for the formation of kaolinite was calculated from the total amount of kaolinite at each temperature (T), based on the assumptions of first-order reaction kinetics and autocatalytic reaction kinetics. The data fit the latter kinetics better than the former. The apparent activation energy

for kaolinite formation from noncrystalline aluminosilicate was calculated from an Arrhenius plot (Figure 7) to be 23.1 and 14.5 kcal/mole for the first-order and autocatalytic kinetics, respectively. These values are similar to data reported earlier for the formation of kaolinite from sericite (17 kcal/mole) (Tsuzuki and Mizutani, 1971).

In nature, spherical halloysite has a similar morphology and composition to this spherical kaolinite. Nagasawa (1978) showed that halloysite formed by alteration of volcanic glass is spherical, whereas that formed by the weathering of rock-forming minerals is tube-shaped. Thus, the dissolution rate of volcanic glass appears to have been faster than that of rock-forming minerals, and the solution around the volcanic glass easily became highly supersaturated. If spherical halloysite precipitated from a highly supersaturated solution as did the spherical kaolinite reported here, the phenomenon described by Nagasawa can be explained.

ACKNOWLEDGMENTS

REFERENCES

Busenberg, E. (1978) The products of the interaction of feldspars with aqueous solutions at 25°C: *Geochim. Cosmochim. Acta* **42**, 1679–1686.

De Kimpe, C. R. and Fripiat, J. J. (1968) Kaolinite crystallization from H-exchanged zeolites: *Amer. Mineral.* **53**, 216–230.

De Kimpe, C. R. and Gastuche, M. C. (1964) Low-temperature syntheses of kaolin minerals: *Amer. Mineral.* **49**, 1–16.

De Kimpe, C. R., Gastuche, M. C., and Brindley, G. W. (1961) Ionic coordination in alumino-silicic gels in relation to clay mineral formation: *Amer. Mineral.* **46**, 1370–1381.

De Kimpe, C. R., Kodama, H., and Rivard, R. (1981) Hydrothermal formation of a kaolinite-like product from noncrystalline aluminosilicate gels: *Clays & Clay Minerals* **29**, 446–450.

De Vijnck, Y. A. (1973) Étude des phases cristallines appartenant au système par Al_2O_3-SiO_2-H_2O formées par traitement hydrothermal de gels obtenus par coprecipitation d'Al(OH)$_3$ et de Si(OH)$_4$: *Silic. Ind.* **38**, 193–211.

Dixon, J. B. and McKee, T. R. (1974) Internal and external morphology of tubular and spheroidal halloysite particles: *Clays & Clay Minerals* **22**, 127–137.

Eberl, D. D. and Hower, J. (1975) Kaolinite synthesis: the role of the Si/Al and (alkali)/(H$^+$) ratio in hydrothermal systems: *Clays & Clay Minerals* **23**, 301–309.

Helgeson, H. C. (1968) Evaluation of irreversible reactions in geochemical processes involving minerals and aqueous solutions—I. Thermodynamic reactions: *Geochim. Cosmochim. Acta* **32**, 853–877.

Helgeson, H. C. (1971) Kinetics of mass transfer among silicates and aqueous solutions: *Geochim. Cosmochim. Acta* **35**, 421–469.

Helgeson, H. C., Garrels, R. M., and Mackenzie, T. (1969) Evaluation of irreversible reactions in geochemical processes involving minerals and aqueous solutions—II. Applications: *Geochim. Cosmochim. Acta* **33**, 455–481.

Hem, J. D. and Lind, C. J. (1974) Kaolinite synthesis at 25°C: *Science* **184**, 1171–1173.

Huang, W. H. and Keller, W. D. (1973) New stability diagrams of some phyllosilicate in the SiO_2-Al_2O_3-K_2O-H_2O system: *Clays & Clay Minerals* **21**, 331–336.

Keller, W. D., Hanson, R. F., Huang, W. H., and Cervantes, A. (1971) Sequential active alteration of rhyolitic volcanic rock to endellite and a precursor phase of it at a spring in Michoacan, Mexico: *Clays & Clay Minerals* **19**, 121–127.

Kirkman, J. H. (1981) Morphology and structure of halloysite in New Zealand tephras: *Clays & Clay Minerals* **29**, 1–9.

Kittrick, J. A. (1970) Precipitation of kaolinite at 25°C and 1 atm: *Clays & Clay Minerals* **18**, 261–267.

La Iglesia, A. and Galan, E. (1975) Halloysite-kaolinite transformation at room temperature: *Clays & Clay Minerals* **23**, 109–113.

La Iglesia, A. and Martin Vivaldi, J. L. (1973) A contribution to the synthesis of kaolinite: in *Proc. Int. Clay Conf., Madrid, 1972*, J. M. Serratosa, ed., Div. Ciencias C.S.I.C., Madrid, 173–185.

La Iglesia, A., Martin Vivaldi, J. C., and Lopez Agayo (1976) Kaolinite crystallization at room temperature by homogeneous precipitation—III: hydrolysis of feldspars: *Clays & Clay Minerals* **24**, 36–42.

La Iglesia, A. and Van Oosterwyck-Gastuche, M. C. (1978) Kaolinite synthesis I. Crystallization conditions for low temperature synthesis with an attempt to calculate the thermodynamical equilibria. Application to laboratory work and field observation: *Clays & Clay Minerals* **26**, 397–408.

Lasaga, A. C. (1981) Rate lows of chemical reactions: in *Kinetics of Geochemical Processes, Reviews in Mineralogy Vol. 8*, A. C. Lasaga and R. J. Kirkpatrick, eds., Mineral. Soc. Amer., Washington, D.C., 1–68.

Linares, J. and Huertas, F. (1971) Kaolinite: synthesis at room temperature: *Science* **171**, 896–897.

Lind, C. J. and Hem, J. D. (1975) Effects of organic solutes on chemical reactions of aluminum: *U.S. Geol. Surv. Water Supply Pap.* **1827G**, 1–83.

Nagasawa, K. (1978) Weathering of volcanic ash and other pyroclastic materials: in *Clays and Clay Minerals of Japan*, T. Sudo and S. Shimoda, eds., Elsevier, Amsterdam, 105–145.

Oberlin, A. and Couty, R. (1970) Conditions of kaolinite formation during alteration of some silicates by water at 200°C: *Clays & Clay Minerals* **18**, 347–356.

Polzer, W. L., Hem, J. D., and Gabe, H. J. (1967) Formation of crystalline hydrous aluminosilicates in aqueous solutions at room temperature: *U.S. Geol. Surv. Prof. Paper* **575B**, 128–132.

Poncelet, G. and Brindley, G. W. (1967) Experimental formation of kaolinite from montmorillonite at low temperatures: *Amer. Mineral.* **52**, 1161–1173.

Rodrique, L., Poncelet, F., and Herbillon, S. (1972) Importance of silica subtraction process during the hydrothermal kaolinitization of amorphous silica-aluminas: in *Proc. Int. Clay Conf., Madrid, 1972*, J. M. Serratosa, ed., Div. Ciencias C.S.I.C., Madrid, 187–198.

Sudo, T. and Yotsumoto, H. (1977) The formation of halloysite tubes from spherulitic halloysite: *Clays & Clay Minerals* **25**, 155–159.

Tomura, S., Shibasaki, Y., Mizuta, H., and Kitamura, M. (1983) Spherical kaolinite: synthesis and mineralogical properties: *Clays & Clay Minerals* **31**, 413–421.

Trichet, J. (1969) Study of the structure of volcanic glass and its relation to the alteration of vitreous rocks: in *Proc. Int. Clay Conf., Tokyo, 1969, Vol. 1*, L. Heller ed., Israel University Press, Jerusalem, 443–453.

Tsuzuki, Y. (1976) Solubility diagrams for explaining zone sequences in bauxite, kaolin and pyrophyllite-diaspore deposits: *Clays & Clay Minerals* **24**, 297–302.

Tsuzuki, Y. and Kawabe, I. (1983) Polymorphic transformations of kaolin minerals in aqueous solutions: *Geochim. Cosmochim. Acta* **47**, 59–66.

Tsuzuki, Y. and Mizutani, S. (1971) A study of rock alteration process based on kinetics of hydrothermal experiment: *Contrib. Mineral. Petrol.* **30**, 15–33.

Tsuzuki, Y., Mizutani, S., Shimizu, H., and Hayashi, H. (1974) Kinetics of alteration of K-feldspar and its application to the alteration zoning: *Geochem. J.* **8**, 1–20.

Tsuzuki, Y. and Suzuki, K. (1980) Experimental study of the alteration process of labradorite in acid hydrothermal solutions: *Geochim. Cosmochim. Acta* **44**, 673–683.

Urabe, K., Ossaka, J., and Yamada, H. (1970) Experimental formation of kaolinite from vermiculite: *Clay Sci.* **4**, 37–44.

Van Oosterwyck-Gastuche, M. C. and La Iglesia, A. (1978) Kaolinite synthesis. II. A review and discussion of the factors influencing the rate process: *Clays & Clay Minerals* **26**, 409–417.

Walter, J. V. and Helgeson, H. C. (1977) Calculation of the thermodynamic properties of aqueous silica and the solubility of quartz and its polymorphs at high pressures and temperatures: *Amer. J. Science* **277**, 1315–1351.